Physical, chemical and optical properties of aerosol particles collected over Cape Town during winter haze episodes

Patience Gwaze[a,b*], Günter Helas[a], Harold J. Annegarn[b], Joachim Huth[c] and Stuart J. Piketh[d]

Airborne measurements were conducted in the winter months of July and August 2003 over the metropolitan area of Cape Town to characterize physical, chemical and optical properties of aerosol particles during intense brown haze episodes. Particles were collected on highly temporally and spatially resolved samples and investigated using a high-resolution scanning electron microscope (SEM). From morphology and elemental composition, particles were categorized in terms of seven groups: aggregated soot particles, mineral dust, sulphates (SO_4^{2-}), sea-salt, tar balls/fly ash, rod-shaped particles associated with soot agglomerates, and those that could not be attributed to any of these groups. Refractive indices of aerosols were derived from chemical distributions obtained from SEM analysis and combined with *in situ* measurements of number–size distributions to determine optical properties of dry particles in the size range 0.1–3.5 μm. Particles exhibited marked spatial and temporal variability in chemical composition. They were externally mixed with highly absorbing soot particles. From number concentrations, light extinction and absorption coefficient ranges were σ_{ep} = 19–755 Mm^{-1} and σ_{ap} = 7–103 Mm^{-1}, respectively (at wavelength λ = 550 nm). Single scattering albedo, ω_0, varied from 0.61 to 0.87 with a mean value of 0.72 ± 0.08; this value was much lower than generally reported in the literature, a result that was attributed to high concentrations of highly absorbing soot (fractional number concentrations of up to 46% were observed in the SEM). The haze could be attributed to extinction of light by fine aerosols composed mainly of anthropogenic particles. High extinction coefficients and low single scattering albedo computed here demonstrate quantitatively the contributions of particulate matter to visibility reduction and the brown haze phenomenon in Cape Town.

Introduction

Cape Town and several other conurbations and industrial areas in South Africa have been identified as environmental 'hotspots' due to persistent high levels of mainly anthropogenic emissions from transport vehicles, and industrial and domestic activities.[1] The city is situated on the southwestern tip of South Africa, with a resident population of just over three million (2001 census).[2] In winter, from May to August and under stable meteorological conditions, Cape Town suffers from episodes of poor visibility due to a brown haze associated with accumulated anthropogenic and natural aerosol particles and trace gas emissions in the boundary layer.[3–6] The creation of the brown haze is linked to the structure and dynamics of the atmospheric boundary layer (ABL), the lower troposphere below 2 km.[5] The term 'brown haze' has been adopted for the more severe pollution episodes, the colour being attributed to enhanced concentrations of highly absorbing soot particles, as opposed to photochemically produced 'white haze' due to highly scattering aerosols.

Studies on Cape Town's brown haze have been conducted to understand the chemical composition of the aerosols involved and to assess the contributions of both particulate matter and trace gases to reduced visibility.[3,4] Winter haze episodes lasting between three and five days were identified from SO_2 and NO_x measurements in 1985/86.[5] As part of an ongoing air quality monitoring exercise, the city authorities measure atmospheric concentrations of PM2.5 and PM10 (particulate matter with aerodynamic diameter of up to 2.5 μm and 10 μm, respectively), H_2S, CO, CO_2, NO_x, SO_2 and VOCs (volatile organic compounds) at strategic locations around the metropolitan area. Annual trends from 1990 to 2002 show that, while averaged concentrations of NO_2 and SO_2 have been steadily decreasing, particulate levels in the central business district (CBD) and Khayelitsha (a formal and informal residential area) have risen.[7] High concentrations of aerosol particles can have considerable effects not only at the local scale (for instance, on health[8] and reduced visibility) but, if transported into the upper troposphere, can affect cloud properties and possibly change the regional climate.[9]

An intensive experiment, known as Cape Town Brown Haze I (CTBH I), was conducted between 1992 and 1996 to determine contributions of major sources to haze and to understand mechanisms of haze formation with the emphasis on visibility effects.[4] Although CTBH I produced some results, characterizing the aerosol particles was limited. This was because the chemical characterization of particulate matter was based on bulk analyses of ground samples collected at selected sites over periods of 24 hours. Such relatively long sampling intervals did not allow for investigation of the highly variable dynamics of the aerosols. Additionally, elemental carbon was shown to be the most significant component of the haze and needed to be further investigated.

As a follow-up to CTBH I, an airborne experiment called Cape Town Brown Haze II (CTBH II) was set up to investigate the atmosphere during intense haze periods in July and August 2003.[6] The main objectives of CTBH II were to: (i) characterize the microphysical, chemical and optical properties, spatial distribution and contributions of aerosol particles to haze;[10] (ii) describe the distribution and contributions of trace gas emissions to haze formation;[11] (iii) identify the importance of VOCs' contribution to local the atmospheric chemistry;[12] and (iv) understand the possible health effects of haze. As a part of CTBH II, the aim of the study reported here is to use microscopic analysis of single particles and *in situ* measurements to characterize the physical (morphology, shape, size, mixing states) and chemical properties of aerosol particles in brown

[a]Department of Biogeochemistry, Max Planck Institute for Chemistry, Mainz, Germany.
[b]Department of Geography, Environmental Management and Energy Studies, University of Johannesburg, P.O. Box 524, Auckland Park 2006, South Africa.
[c]Department of Particle Chemistry, Max Planck Institute for Chemistry, Mainz, Germany.
[d]Climatology Research Group, University of the Witwatersrand, Private Bag 3, WITS 2050, South Africa.
*Author for correspondence. E-mail: pgwaze2@yahoo.com

Table 1. Flight numbers, dates in 2003, times and ground locations overflown during the collection of the ABS aerosol samples.

Flight number and time	ABS sample ID	Ground locations flown over during sampling
Flight 9, 6 August 10:20–12:00 UTC*	Sample 1	Several turns over the central business district (CBD) to Pinelands
	Sample 2	Goodwood, Pinelands to Wynberg
	Sample 3	Wynberg, Grassy Park, Mitchells Plain
	Sample 4	Khayelitsha, Mfuleni, Bellville
Flight 13, 13 August 12:30–15:00 UTC	Sample 5	Ysterplaat to Mitchells Plain and Cape Town International Airport runway
	Sample 6	Goodwood to Wynberg
Flight 14, 22 August 07:20–09:00 UTC	Sample 7	Goodwood, Belhar, Manenburg, Wynberg
	Sample 8	Mitchells Plain over sea to Fish Hoek
	Sample 9	Several turns over Khayelitsha
	Sample 10	Several turns around industrial site B and Bellville
Flight 16, 23 August 06:30–08:40 UTC	Sample 11	Malmesbury to Robben Island
	Sample 12	Ysterplaat and central business district

*Universal Time Coordinated, which is two hours behind local time in Cape Town.

haze. Using an approach similar to that described by Ebert *et al.*,[13] complex refractive indices of aerosols were quantified from highly resolved spatial and temporal measurements taken from aircraft. Aerosol optical properties (single scattering albedo, and extinction coefficients) were quantified to show the contributions of particulate matter to visibility reduction. This study is the first of its kind to provide quantitative and qualitative descriptions of the microphysical and optical properties of anthropogenic aerosol particles and their effects on visibility in a South African city. An account of number concentrations and spatial distributions of particles is in preparation (Gwaze *et al.*).

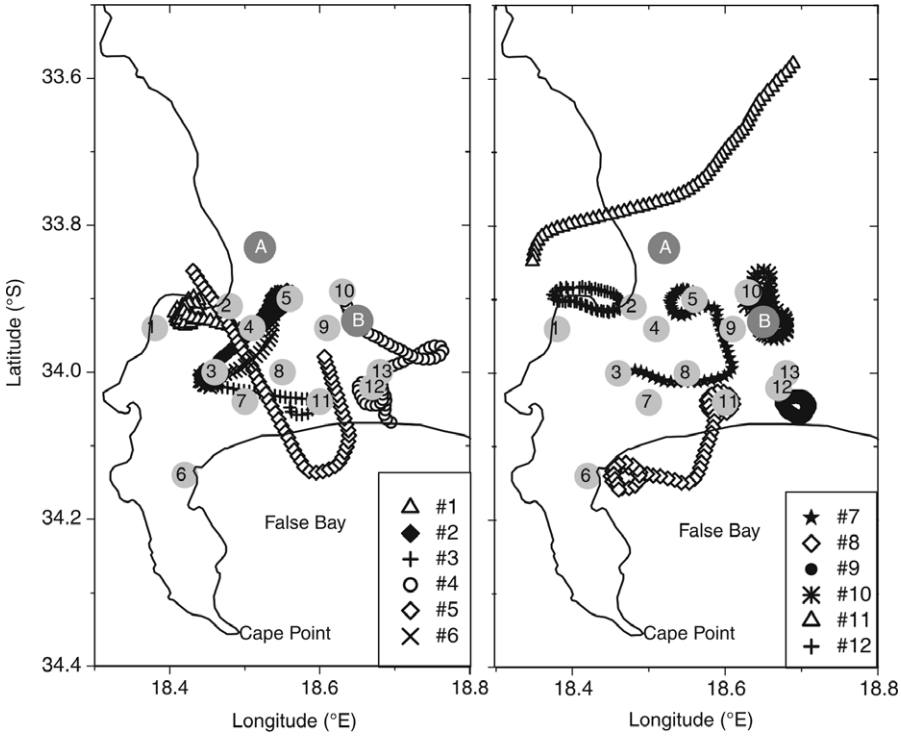

Fig. 1. Flight segments for which ABS aerosol samples were collected for SEM analysis on flights 9, 13, 14 and 16 on 6, 15, 22 and 23 August, respectively. Numbered locations are schools that were used to identify the aircraft's global position system with ground locations, where: 1, Camps Bay; 2, Ysterplaat; 3, Wynberg; 4, Pinelands; 5, Goodwood; 6, Fish Hoek; 7, Grassy Park; 8, Manenburg; 9, Belhar; 10, Bellville; 11, Mitchells Plain; 12, Khayelitsha; 13, Mfuleni. Industrial sites A and B are an oil refinery and a glass manufacturer, respectively. Only partial flight paths are shown, for reasons of clarity.

Experimental

Aerosol measurements

Airborne sampling of aerosol particles and online measurements of trace gases were conducted over the Cape Town metropolitan area in South African Weather Service's twin-prop Aerocommander 690A ZS-JRB. This aircraft has an operational ceiling of 4 km and maximum speed of 200 m s^{-1}. Seventeen flights, confined to altitudes below 2000 m, were conducted between 29 July and 26 August 2003, with a total flying time of approximately 24 hours. Based on the diurnal development of the atmospheric boundary layer, flights were conducted at different times of the day in order to contrast measurements of particle properties in the mornings and afternoons on haze and non-haze days. Morning flights were undertaken to sample relatively fresh haze concentrated close to the ground. Afternoon flights sampled 'matured' haze which had become mixed within the convective boundary layer, and possibly transported laterally. Four flights were selected as case studies for this paper, flights 9, 13, 14 and 16 conducted on 6, 15, 22 and 23 August. The flight details are given in Table 1.

The aircraft carried instruments for measuring aerosol particles and trace gases. Filter samples of aerosol particles were collected using an Air Borne Streaker (ABS) sampler, a device described in detail elsewhere.[14] The ABS collects aerosol samples on temporally and spatially resolved individual deposition spots on a rotating wheel. The particles are collected isokinetically with a 10-μm cut-off diameter onto straight-through polycarbonate membrane filters with a pore size 0.3 μm. The ABS could sample between 45 and 60 litres of air for each spot, with a flow rate of 4.5 ± 0.5 l min^{-1}. Stepping time intervals of the wheel were controlled either manually or in an automated mode using a microprocessor. Collection times for each deposition sample were manually correlated with the aircraft's navigation system, and regularly checked and synchronized to within a certainty of ± 30 seconds. Figure 1 shows flight segments in which the 12 ABS samples analysed in this study were collected. Numbered locations are schools that were used to correlate the aircraft's global positioning system with ground locations. The location names are given in the figure caption. Two major industrial sites, A and B, are an oil refinery and a glass manufacturing company, respectively.

A Passive Cavity Aerosol Spectrometer Probe (PCASP–100X, PMS Inc., Boulder, Colorado) was used to measure number–size

distributions of dry aerosol particles with optical diameters of 0.1 to 3.5 μm in 15 size categories. An inlet heating system prevented icing, hence particles were dehydrated before size measurements. The PCASP was calibrated using latex spheres and shifts in size bins were adjusted in terms of them.[10] Sizes in the PCASP were determined assuming that light has been scattered by homogeneous spherical particles of refractive index $m = 1.585 - 0i$. However, atmospheric particles have different refractive indices, shapes, mixing states and associated water, hence the PCASP size measurements had to be adjusted to represent ambient particles. Discussions of such effects are beyond the scope of this paper; details can be found elsewhere.[10,15]

Microscopy analyses

Twelve ABS spots collected from the case studies were selected and identified as samples 1 to 12 as indicated in Table 1. The ABS samples were analysed for morphology, size distributions and elemental composition of individual aerosol particles using a high-resolution field emission scanning electron microscope (Leo 1530 SEM, E.M. Ltd., Cambridge, England, now Nano Technology Systems, Zeiss). Elemental compositions of particles were determined by an energy-dispersive X-ray (EDX) analysis. Although the EDX is able to detect the light elements C, N and O, the spectra were contaminated by background signals of C and O from the filter substrate. EDX analyses therefore provided semi-quantitative information on the elemental composition of particles, excluding light elements. To image particles (or analyse particles with EDX), random trajectories were followed on several positions on each deposited sample to avoid operator bias and non-uniform deposition. Several images were taken for each sample to obtain reasonable statistical counts of particles. Sparse deposits on substrates and errors due to overlapping particles were negligible. Filters were not coated to enhance electrical conductivity and image contrast (as is common with non-conductive substrates) because the coating would have interfered with the measurements.

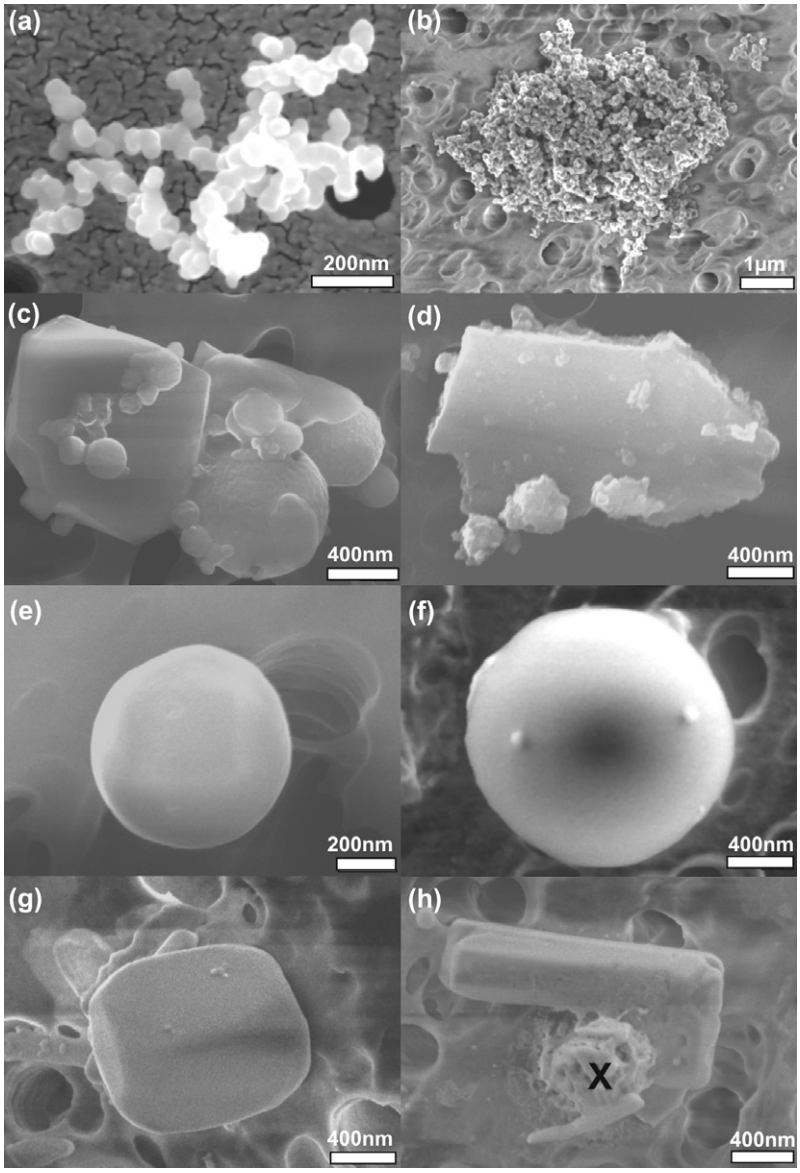

Fig. 2. Typical images of particles identified in SEM analyses: (**a**) loose soot aggregate which was collected with a ground sampler, whose morphology is similar to those aggregates collected on the aircraft; (**b**) large and compact soot aggregate; (**c**) agglomerate of mineral dust particles with complex composition of Na, Si, Ca, Fe, Zn, and Mn and traces of S, Mg and Al; (**d**) iron silicate dust particle; (**e**) tar spheroid of 0.68 µm diameter; (**f**) large spherical fly ash particle with a surface diameter of 1.59 µm; (**g**) euhedral sea-salt particle; (**h**) an aged sea-salt particle with a halo (around X) of liquid, which was highly volatile in the electron beam.

Particle morphologies were identified from SEM images. Based on these and elemental composition, particles were categorized in terms of seven groups, as follows: aggregated soot particles, mineral dust, sulphates (SO_4^{2-}), sea-salt, tar balls/fly ash, and rod-shaped particles (some were associated with soot agglomerates); those that could not be attributed to any of these categories were labelled 'others'. All visible particles on selected images were counted, with total number counts N_A of 731, 630, 492, 1410, 271, 297, 589, 388, 671, 954, 114 and 157 particles on samples 1 to 12, respectively. In total, 6704 particles were manually identified and placed variously in the seven groups.

Aerosol chemical composition and particle morphology

Typical SEM images of aerosol particles are shown in Figs 2 and 3. The relative abundances of the particles by category are plotted in Fig. 4(a). Soot particles were the most prevalent type in the boundary layer. These were identified as agglomerates of small, nearly spherical primary carbonaceous particles. The

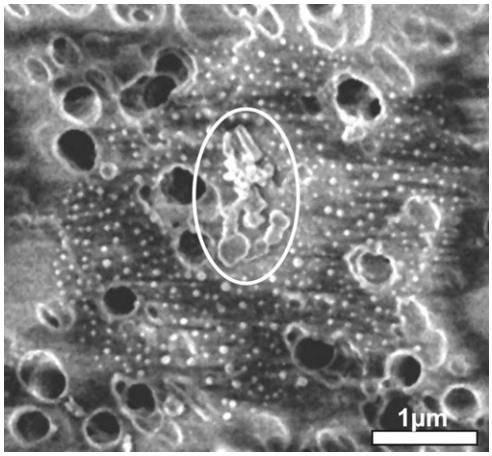

Fig. 3. Sulphate particle with a satellite scatter of sulphate crystals formed from the dehydration of a sulphate droplet. Morphologies of encircled core particles varied from clusters to single large amorphous grains clearly larger than the satellite droplet crystals.

compactness of soot aggregates varied from chained, branched assemblages as shown in Fig. 2(a) to closely packed particles illustrated in Fig. 2(b). Some aggregates were formed with large spherical particles of more than 100 nm diameter—these are probably tar balls[16] that were embedded in soot particles during the coagulation process in cooling smoke. The contributions of soot particles varied significantly from location to location, indicating localized, possibly point sources within the Cape Town area. The fractional contributions varied from 12% to a peak of 46% observed for sample 11 collected on Flight 16. Locations like the CBD, Goodwood and Pinelands were associated with the highest soot concentrations, mainly from vehicle emissions; and Khayelitsha, where soot particles were emitted largely by domestic fires. Fractional number concentrations of soot particles were highest on days with the lowest relative humidity. Such high soot contributions match studies of other urban environments where externally mixed soot dominated the light absorbing component of urban aerosols.[17,18] The mass contribution of elemental carbon in central European studies was 10–31% (for particle diameters of 0.05–1.20 μm).[19] Higher proportions have been reported at an urban site in Japan, where soot particles with diameter range 0.08–1.60 μm were present in 42–49% of the fractional number concentrations.[18] In the diameter range 0.1–0.2 μm, urban polluted air masses at a rural site in Germany consisted of up to 80% soot.[20] (Soot contributions in our study might have been slightly overestimated because soot particles were stable both under the electron beam and in the SEM vacuum unlike secondary derived aerosols, which might have sublimated and were therefore not accounted for.) Mixed particles were considered for combined soot/sea-salt, soot/mineral dust or soot/sulphates. Soot particles observed in our study were externally mixed, suggesting either fresh emissions of particles that had not been aged by coagulation, restructuring, gas uptake or chemical reactions. Soot particles spend considerable time after emission before subsequent interaction in the atmosphere.[21]

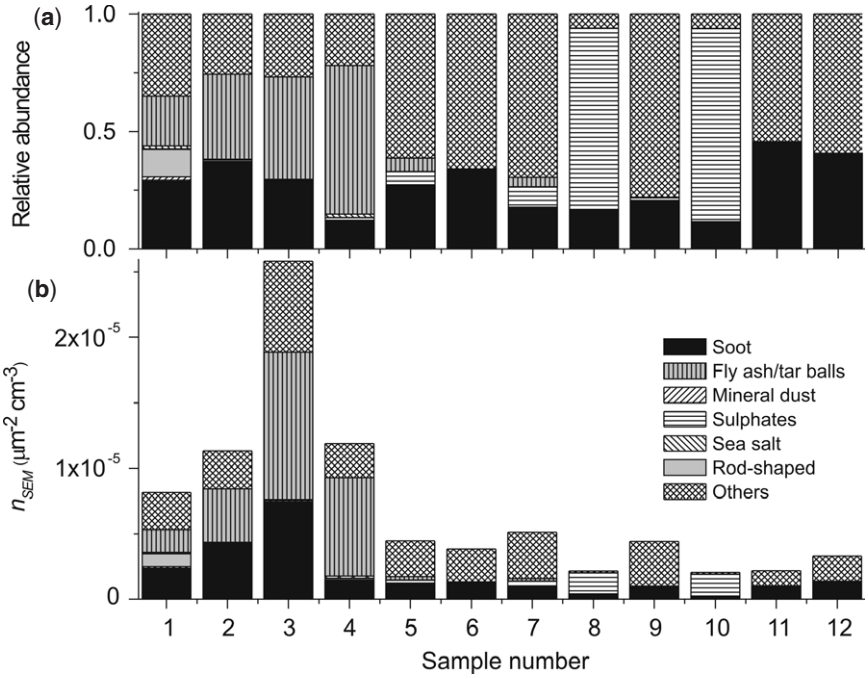

Fig. 4. (**a**) Relative contributions of seven particle groups identified by SEM analysis. The samples were collected on Flight 9 (samples 1–4), Flight 13 (samples 5 and 6), Flight 14 (samples 7–10) and Flight 16 (samples 11 and12). (**b**) Surface-number density of particles deposited on the ABS filters. These densities were calculated from the particles counted, total area on SEM images and volume sampled per deposition spot by assuming a collection efficiency of 100%.

Mineral dust particles were identified both from their morphology and elemental compositions. Figures 2(c) and (d) show some typical examples. Coarse particles were relatively abundant, with morphologies that varied from agglomerates of spheroids with diameters between 20 nm and 1 μm to crystalline particles with sharp edges. EDX spectra of several particles from all samples show that they consisted mainly of Na, Mg, Al, Si, K, Ca, Ti, Fe and Zn. The maximum fractional number concentration of dust particles on all samples was less than 2%. Such low proportions are to be expected in Cape Town samples collected in winter, which is also the wet season, because the sources of these particles, exposed land surfaces and vehicle emissions, are relatively weak. In a previous study during the winter of 1992,[3] average elemental concentrations of mineral dust over Cape Town analysed by PIXE (proton-induced X-ray emission) indicated that dust particles contributed less than 5% of total mass. Our study therefore indicates higher fractional mass of mineral dust content than has previously been reported.

All individual spherical particles were identified as tar balls and fly ash, of which typical SEM images are illustrated in Figs 2(e) and (f). Without information on each individual particle's chemistry, it is not possible in this study to identify these particles individually owing to the overlap in size and similarity in morphologies. Of the few large spheroids analysed with EDX, however, tar balls were identified as mainly carbonaceous particles, whereas fly ash contained traces of metallic elements. Tar balls are formed in smouldering fires, and their presence signifies biomass burning as a source,[16] probably from domestic wood fires. Fly ash particles are formed by vaporization and condensation of mineral components in the fuel, particularly coal and peat, during combustion.[22] The main sources of Cape Town's fly ash are likely to be industrial combustion processes. Other particles identified were rod-shaped with a 12% relative abundance (sample 1 only). Some of these particles were associated with both compact and branched soot aggregates and were stable in the SEM beam. It is possible that these particles were particulates generated by combustion and embedded in soot particles during coagulation in the cooling smoke.

Euhedral tabular particles were identified as sea-salt, examples of which are illustrated in Fig. 2(g) and (h). Aged particles were volatile in the SEM beam. The particle labelled X in Fig. 2(h) had a halo from the dehydration of the deliquescent component of the particle after deposition on the filter. Contributions of aged sea-salt particles on all samples were negligible—only two particles were identified from 6704 analysed; the maximum contribution of both fresh and aged sea-salt particles was 1.4%. As noted in an earlier study,[4] Cape Town is not subjected to aged or fresh marine air masses with high sea-salt particle loadings during intense haze episodes.

Sulphate particles were identified by a scatter of small, nearly spherical 'satellite' droplets around central core particles (Fig. 3). The particles were most abundant on Flight 14, with fractional number concentrations of up to 82% on sample 10. Surface diameters of satellite particles were between 60 and 200 nm (measured on 550 particles). The particles were spread over several square micrometres and this area possibly depended on

the size and dilution of the deposited material. The satellite particles were sensitive to the SEM electron beam and sublimated entirely and more rapidly than the core particles. The morphology of the central cores varied from spheres clearly larger than the satellite droplets, to small clustered particles to single amorphous grains up to 0.5 μm in size. Some amorphous grains might not have completely dissolved upon deposition or sulphates had condensed on existing particles. Similar morphologies of sulphates (satellite rings with cores) have been observed on microscope images elsewhere.[23–25] In those studies, satellite droplets were identified from electron diffraction patterns as sulphate crystals formed from the dehydration of sulphate droplets.

Particles labelled 'others' were difficult to categorize in terms of any of the groups discussed above because of their indistinguishable morphologies. Since Cape Town is dominated by aerosol particles from local anthropogenic sources,[4] 'other' particles are likely to be mixed grains, organic carbonaceous aerosols or nitrates—essentially, photochemically produced secondary aerosols derived from gaseous precursors or particles that have aged. Local emissions can accumulate over the study area for three to five days because of stable meteorological conditions, before they are removed by wet deposition.[5] During this time, particles might undergo ageing that leads to the formation of new particles with morphologies different from externally mixed particles categorized in one of the six other groups discussed above.

The surface-number density of particles deposited on the ABS filters, n_{SEM} (μm^{-2} cm^{-3}), were calculated from counted particles N_A and total area A on SEM images by assuming a maximum collection efficiency of 100% on the ABS samples and normalized to the volume sampled V_t, where $n_{SEM} = N_A / (A \times V_1)$. Figure 4(b) shows n_{SEM} values and contributions of each particle group. The highest surface-number densities were observed for samples 1–4, particularly sample 3. Although not shown here, these densities were well correlated with the normalized averaged PCASP number concentrations, N_{PCASP}, measured over the same time intervals, with a linear correlation coefficient of 0.82.[10] Further comparisons between these number concentrations are beyond the scope of this paper and are discussed elsewhere.[10]

Relative abundance of particles

Figure 4 shows fractional contributions of seven particle groups for samples 1–12. Aerosols collected within haze layers on three flights will now be discussed in detail.

Flight 9 recorded the highest particle concentrations in the boundary layer. Combustion-generated aerosols dominated particle number concentrations in all samples, with total fractional values of between 65% and 80%. There was marked spatial variability in the composition of these particles: soot particles ranged from 12% to 37%, tar balls/fly ash particles from 21% to 63%, and rod-shaped particles up to 12%. These variations indicate two main differences among their sources. First, soot particles in samples 1–3 can be attributed to vehicle emissions from the CBD, Goodwood and Pinelands areas; they are more than double the proportion from Khayelitsha (sample 4). Second, the highest concentrations of tar balls/fly ash particles were collected over the residential areas of Khayelitsha, Mfuleni and Bellville, areas where domestic fires were dominant.

The particles collected on Flight 14 were dominated by externally mixed soot aggregates and sulphate particles. The averaged fractional contribution of soot particles was 17%, the lowest for the four flights considered here. Sulphates were highly variable, with fractional concentrations of between 9% and 82%. These high sulphate loadings are likely to be secondary combustion products of anthropogenic SO_2. The emissions need to spend considerable time in the atmosphere to be photochemically transformed to sulphates.[26] Additionally, SO_2 is highly soluble in water and any hydrated particles present might have provided surfaces for the efficient conversion of SO_2 to sulphates. While natural sulphates might also be present, particularly at a coastal location like Cape Town, they are outweighed by anthropogenic sources.[27]

Both samples collected on Flight 16 were dominated by soot particles with fractional concentrations of 46% and 41%, respectively. Although sample 11 was collected in what would have been expected to be relatively cleaner air than for sample 12, the soot contributions indicate how anthropogenic emissions influence on the regional atmosphere over Cape Town. The average fractional concentrations of soot increased between 22 and 23 August from 17% to 43%, whereas sulphate contributions declined from 82% to none. Because most aerosol sources identified in CTBH I were habitual with diurnal patterns, differences in aerosol compositions between these two days can be attributed to variations in meteorological conditions; 23 August was relatively dry in the boundary layer, unlike the day before.[28] Sulphate concentrations have been observed to increase with ambient humidity,[29] so the differences between 22 and 23 August might indicate the dependence of sulphate contributions on prevailing humidity. The production of sulphates over Cape Town may therefore be suppressed on those days due to the generally dry conditions associated with intense haze episodes.

Backward trajectory analysis indicated that air masses arriving at Cape Town during the measurement periods originated at high altitudes from a clean background atmosphere with limited continental influence.[10] Aerosol loadings over the city were therefore dominated by emissions from local sources. The chemical compositions of aerosols displayed large variations both temporally and spatially, which indicated that the mixing of the boundary layer by horizontal advection was relatively poor.

Aerosol optical properties

Refractive index

We defined complex refractive indices of aerosols in terms of the chemical compositions, abundance and mixing states of the particles involved using an approach similar to that described by Ebert *et al.*[13] This index is a fundamental aerosol parameter that describes the optical properties of particles and depends on their chemical composition and the wavelength of incident light. Refractive indices were chosen for externally mixed chemical species with refractive indices $m_j = n_j - ik_j$ for groups $j = 1$ to 7 at a wavelength of 550 nm. Refractive indices of soot particles given in the literature vary widely from $m = 1.5 - 0.47i$ (ref. 30), $m = 1.75 - 0.44i$ (ref. 31) to $m = 1.96 - 0.66i$ (ref. 26), because of variable internal molecular structures and substances that might be adsorbed on the soot particles.[30] A wavelength-dependent refractive index given by d'Almeida[31] was chosen because it is representative of anthropogenic soot with a high absorbing component. Sulphate particles were treated as freshly formed H_2SO_4 with a refractive index of $m = 1.43 - 0.0i$, and sea-salt particles were taken to be pure sodium chloride with $m = 1.54 - 0.0i$.[26] A refractive index of $m = 1.56 - 0.006i$, representative of crustal material whose composition might be variable, consisting mainly of silicates, oxides and hydroxides of several metals, was chosen for mineral dust particles.[32] The index is more suit-

Table 2. Effective refractive indices determined from SEM analyses (at λ = 550 nm) and optical properties of particles computed from maximum and mean number concentrations measured by the PCASP.

Sample ID	Refractive index		Maximum number concentrations					Mean number concentrations					
	n_I	k_I	σ_{ep} (Mm^{-1})	σ_{ap} (Mm^{-1})	ω_0	V ($\mu m^3\ cm^{-3}$)	N (cm^{-3})	σ_{ep} (Mm^{-1})	σ_{ap} (Mm^{-1})	ω_0	V ($\mu m^3\ cm^{-3}$)	N (cm^{-3})	Altitude ± s.d. (m a.s.l.)
Sample 1	1.57	0.18	163.7	56.6	0.65	53.30	6279	32.12	12.68	0.61	8.42	1624	355 ± 155
Sample 2	1.59	0.16	119.1	42.5	0.64	29.39	5273	31.05	11.46	0.63	7.67	1607	280 ± 109
Sample 3	1.57	0.13	173.4	57.2	0.67	32.03	8897	95.12	30.32	0.68	20.45	4748	130 ± 12
Sample 4	1.53	0.05	368.5	47.1	0.87	98.64	8555	27.16	4.06	0.85	8.04	1669	269 ± 126
Sample 5	1.56	0.12	82.6	22.0	0.73	16.47	3631	18.79	4.93	0.74	5.49	835	1068 ± 641
Sample 6	1.59	0.15	18.9	7.3	0.61	3.41	1278	13.81	4.28	0.69	4.47	606	227 ± 209
Sample 7	1.54	0.08	79.0	20.8	0.74	16.96	7751	15.14	3.27	0.78	4.14	1022	143 ± 49
Sample 8	1.49	0.07	265.1	53.7	0.80	54.33	7702	32.02	6.01	0.81	9.24	1198	111 ± 67
Sample 9	1.55	0.09	201.0	51.1	0.75	36.69	11175	20.97	4.46	0.79	5.88	962	190 ± 18
Sample 10*	1.47	0.05	755.1	103.0	0.86	162.61	16172	17.90	2.66	0.85	5.95	951	261 ± 44
Sample 11	1.61	0.20	41.8	15.7	0.62	11.55	1774	21.84	7.85	0.64	6.95	807	166 ± 49
Sample 12	1.61	0.18	61.6	17.4	0.72	34.30	1751	27.10	8.62	0.68	9.49	945	136 ± 13
Mean	1.56	0.12	194.2	41.2	0.72	45.81	6686	26.90	7.14	0.76	7.50	1292	
s.d.	0.04	0.05	194.6	25.4	0.08	42.72	4182	19.42	6.99	0.10	3.85	992	

*Sample 10 was collected inside an industrial plume.

able for these investigations, as evidenced from EDX analyses of individual dust particles. For tar balls/fly ash, rod-shaped particles and for the group of particles labelled 'others', we used a refractive index for a non-absorbing aerosol of $m = 1.5 - 0.0i$.[33] It was assumed that the main absorbing component of all aerosols collected was soot, and that mineral dust particles were weakly absorbing.

Effective refractive indices $m_I = n_I - ik_I$ of samples 1–12 were calculated using the volume averaging mixing rule.[33] Particles were externally mixed and therefore number distributions of each particle group $j = 1$ to 7 were weighted against corresponding fractional abundance in Fig. 4 by assuming size-independent fractional compositions with $m_j = n_j - ik_j$ and particle volume V_j. The effective complex refractive index is given by

$$m = \frac{n_1V_1 + n_2V_2 + \ldots n_7V_7}{V_1 + V_2 + \ldots V_7} - i\frac{k_1V_1 + k_2V_2 + \ldots k_7V_7}{V_1 + V_2 + \ldots V_7}. \quad (1)$$

Representative refractive indices are listed in Table 2. The real parts n_I varied from 1.47 to 1.61. The complex components k_I varied from 0.05 to 0.20, depending on the fractional percentage of soot particles, with a mean effective refractive index of $m = 1.56 - 0.12i$. While the range of the real component is in agreement with values of n_I quoted in the literature, the imaginary component k_I is much larger than observed for aerosols influenced by urban pollution or biomass burning.[17,34] As seen from the variations in $m_I = n_I - ik_I$ in Table 2, a single complex refractive index of $m = 1.50 - 0.1i$ recommended for polluted urban areas[33] cannot be applied to Cape Town, because there are strong spatial and temporal variations in contributions of particle species. Because highly absorbing soot particles vary greatly in concentration, deviations from the effective refractive indices will result in large uncertainties in calculating optical properties of aerosols in some locations, particularly absorption coefficients and single scattering albedo, parameters which are most sensitive to refractive indices assigned to the aerosol.

Optical properties

The optical properties of dry particles were determined for those segments of flight tracks corresponding to sampling times of ABS deposition spots investigated with the SEM. Aerosol refractive indices were derived from the chemical composition of particles in the SEM analyses; particle number concentrations, N_{PCASP} (cm^{-3}), were measured *in situ* with the PCASP in the size range 0.1–3.5 μm. Particles were dry because the heating system in the PCASP inlet was switched on. We were not able to calculate aerosol number concentrations from SEM observations.[10,20]

Extinction coefficients σ_{ep} (the sum of scattering and absorption coefficients, σ_{sp} and σ_{ap}, respectively) and single scattering albedo (ω_0) were calculated with a Mie scattering routine at light wavelength λ = 550 nm for homogeneous and spherical particles ensembles.[35]*

Parameters were computed as

$$\sigma_{ep} = \sum_{j=1}^{7}(\sigma_{sp,j} + \sigma_{ap,j}) \quad (2)$$

$$\omega_0 = \frac{\sum(\sigma_{sp,j} + \sigma_{ap,j})*\omega_j}{\sum(\sigma_{sp,j} + \sigma_{ap,j})}, \quad (3)$$

where j = 1 to 7 are the various particle groups. Extinction coefficients are additive.[33] The composite single scattering albedo ω_0 was determined on the basis of weighted contributions of each chemical species.[36]

There was strong spatial variability of particle number concentrations. To give an overview of optical properties, therefore, parameters were computed from point measurements of maximum and mean PCASP number concentrations (N_{PCASP}) probed during collection of each ABS sample. The maximum number concentrations was representative of concentrations observed in the most-polluted locations within the boundary layer.[10] Although the volume distributions would be more appropriate in defining ranges of optical parameters (because optical properties are sensitive to particle volume rather than number concentrations), the concentrations of particles larger than 1 μm were very low, and volume distribution might have been biased by the poor detection of the PCASP at low concentrations. Optical parameters derived for maximum number concentrations are given in Table 2. These optical properties will now be discussed in terms of N_{PCASP}.

Scattering and absorption coefficients

The range of light extinction coefficients of particles was 19–755 Mm^{-1} (mean σ_{ep} = 194 ± 195 Mm^{-1}) and of absorption coefficients was 7–103 Mm^{-1} (mean σ_{ap} = 41 ± 25 Mm^{-1}; the unit Mm^{-1} represents inverse megametres = 10^{-6} m^{-1}). Extinction and absorption coefficients from the mean N_{PCASP} were σ_{ep} = 29 ±

*The extinction coefficient defines the fractional depletion of light per unit thickness of an aerosol due to scattering and absorption by particles. The single scattering albedo is the ratio of scattering coefficient to extinction coefficient ($\omega_0 = \sigma_{sp}/\sigma_{ep}$), an optical parameter which gives information on the radiative forcing of an aerosol.

21 Mm^{-1} and $\sigma_{ap} = 8 \pm 7\ Mm^{-1}$ and up to 14 factors less than those derived from the maximum number concentrations. Extreme values of $\sigma_{ep} = 755\ Mm^{-1}$ and $\sigma_{ap} = 103\ Mm^{-1}$ for sample 10 were observed at low altitudes directly over industrial site B (a glass manufacturer). These measurements probably corresponded to the plume of stack emissions from the factory, and the magnitudes are not representative of the brown haze overall. From the maximum number concentrations, the atmosphere over Khayelitsha (samples 4 and 9) showed the highest aerosol volume and hence more light extinction. However, considering the mean number concentrations, it is the CBD and areas west of Khayelitsha that demonstrated the highest average extinction coefficients (samples 1, 3 and 12).

Extinction coefficients for Cape Town air are much higher than expected for clean and average background continental conditions, for which σ_{ep} values are 23 Mm^{-1} and 57 Mm^{-1}, respectively. The extinction coefficients are an order of magnitude larger than Rayleigh extinction by gases, indicating the dominance of particles in light extinction.[26] During haze episodes, the mean magnitude of σ_{ep} observed for Cape Town was higher than the corresponding figures from studies at European and American urban sites. Scattering and absorption coefficients measured in Atlanta were σ_{sp} (λ = 530 nm) = 121 ± 48 Mm^{-1} and σ_{ap} = 16 ± 12 Mm^{-1}, respectively.[37] Scattering coefficients on coastal and surrounding areas influenced by urban–industrial emissions from Marseilles were between 35 ± 28 Mm^{-1} and 63 ± 43 Mm^{-1} depending on the prevailing breeze, and σ_{ep} was overall less than 100 Mm^{-1}.[38] Three-year mean values of σ_{ep} for several U.S. locations were lower than 164 Mm^{-1}.[39] However, coefficients in our study are less than those observed for Beijing, where mean scattering coefficients of 488 ± 370 Mm^{-1} and absorption coefficients of 83 ± 40 Mm^{-1} have been reported.[40]

Extinction coefficients in this study were computed for dry particles at relative humidity (RH) of 30–40% in the PCASP, a humidity range assumed by several researchers when the heating system is on.[34,41] In higher ambient humidity, scattering is enhanced by the growth of hygroscopic particles. Unless coated by hygroscopic material, soot, tar balls/fly ash, and mineral dust particles are non-hygroscopic and were probably dry at RH = 35%. Sea-salt particles were treated as NaCl with deliquescence relative humidity (DRH) 75% and were therefore crystalline in the PCASP.[26] Sulphate particles (treated as H_2SO_4) are highly hygroscopic,[42] however, hence they contained water during size measurements. Owing to the presence of sulphates, ambient extinction coefficients might have been higher on samples 8 and 10, while being negligible on the rest of the samples. Absorption coefficients would not be altered by humidity growth, however, since freshly emitted soot particles, identified as a significant absorbing component of the aerosols, do not exhibit considerable growth. Rather, particles initially collapse with increase in humidity.[43]

Single scattering albedo

Computed values of single scattering albedo, ω_0, varied from 0.61 to 0.94, with a mean value of 0.72 ± 0.08. The lowest ω_0 values were observed on Flights 9, 13 and 16 (6, 15 and 23 August, respectively). The magnitude of ω_0 indicates a large absorption component, due to high fractional number concentrations of soot particles. By assuming internally mixed particles with the same volume of absorbing soot, the mean ω_0 value was 0.60 ± 0.10, and much lower than that of externally mixed aerosols. This is because for internal mixtures, the entire particle volume absorbs radiation rather than a fraction that is composed of soot. The difference in ω_0 between the two mixing states illustrates the significance of using single particle analyses instead of bulk chemical analyses to describe the aerosol mixing conditions completely.

The range of ω_0 calculated here is comparable to magnitudes derived from *single particle analyses* elsewhere. By determining size-resolved chemical compositions in SEM analyses, ω_0 of 0.62–0.76 was derived for externally mixed urban aerosols in central Europe.[20] However, from *direct* optical measurements, mean ω_0 values observed from other techniques are higher than the Cape Town figure. A mean ω_0 of 0.83 was observed during the summer in central Europe.[19,44] During INDOEX (Indian Ocean Experiment), anthropogenic aerosol advected from the continent attributed to an absorption component with ω_0 between 0.6 and 0.8.[45] The single scattering albedo of anthropogenic influenced aerosols in the boundary layer determined during ACE-2 (North Atlantic Aerosol Characterization Experiment) was higher than 0.83.[46] Generally, mean magnitudes of $\omega_0 > 0.8$ are reported for European, U.S. and east Asian cities.[9,33,37,38,40]

Sensitivity studies were conducted in the following way to examine why the mean value of ω_0 in our study was considerably lower than the values of single scattering albedo in the literature. First, on the assumption that fractional contributions of soot particles were overestimated, because volatiles were lost or other particles were not fully accounted for in the SEM analyses, optical parameters were computed with 10% and 20% less soot on all samples. The mean scattering albedo then increased only from 0.72 to 0.74 and 0.75, respectively, indicating that absorption coefficients were not significantly sensitive to overestimations within 20%, an acceptable experimental error margin in SEM analysis. Second, there are limitations in defining particle size with the PCASP due to effects of aerosol refractive indices. Without this correction, light scattering coefficients derived from the PCASP size distributions were systematically lower (by up to a factor of 2) than those measured by a nephelometer.[15] These corrections were not carried out here because size-resolved relative abundances of particle groups are unknown.

Third, extinction coefficients and ω_0 might have been underestimated due to size truncation by the PCASP.[10] Fourth, the main absorbing particles were taken to be soot and mineral dust particles. If soot particles or iron oxides were incorporated into the 'others' group, ω_0 and σ_{ap} might be lower than has been computed. If 'others' contained more scattering aerosol, extinction coefficients and ω_0 calculated here might be underestimated. Finally, the approach of determining complex refractive indices from SEM analysis is applicable only to dry aerosols because water and other volatiles are lost in the SEM vacuum. PCASP sizes were measured at less than 40% relative humidity, and below the DRH of most particle groups identified. An attempt to correct for hygroscopic growth was made to represent ambient sulphates aerosols.[10] The mean ω_0 increased from 0.79 ± 0.10 to 0.82 ± 0.09, a small change compared to the deviation of ω_0. It should be emphasized, however, that while most optical parameters in the literature are column integrated values, optical parameters computed in our study are *in situ* measurements recorded inside pollution strata.

Despite the uncertainties in PCASP size distributions and SEM analyses mentioned above, lower ω_0 observed here might also indicate the apparent differences in emission control regulations of vehicles and industry between Europe, the U.S. and South Africa. Vehicle emissions, particularly from diesel engines, were observed to contribute up to 60% of the PM2.5 fraction in Cape Town air.[4] Up to 41% of the particulate matter emitted by

diesel engines is in the form of highly absorbing soot particles.[47] It is therefore reasonable to conclude that soot particles contribute to a large light-absorption component in Cape Town's air and so the aerosol single scattering albedo is expected to be lower than observed in Europe and America.

Conclusions

The physical and chemical properties of aerosols were investigated from an aircraft during brown haze episodes in Cape Town. An Air Borne Streaker sampling technique combined with scanning electron microscopy offered a novel approach to describing the highly variable chemical compositions of these atmospheric particles. The contributions of soot particles were enhanced around localized sources. The city's CBD and Khayelitsha contributed large amounts of soot from mobile sources, and industrial and domestic fuel burning. Soot particles were externally mixed, typical of freshly emitted particulates, with fractional contributions of up to 46%. Owing to their large surface areas, such high concentrations of soot particles are likely to enhance heterogeneous reactions in the polluted atmosphere of Cape Town. Sulphate particles were found in fractional concentrations of 0–82%. However, sulphate production might be supressed as a result of the dry conditions associated with intense haze episodes.

The complex refractive indices of aerosols were computed from the relative abundance of the seven particle groups identified by SEM analysis. These indices were combined with PCASP size distributions to quantify the optical properties of aerosols. From *in situ* number concentrations that corresponded to pollution episodes, the ranges of light extinction and absorption coefficients of particles were $\sigma_{ep} = 19–755\ Mm^{-1}$ and $\sigma_{ap} = 7–103\ Mm^{-1}$, respectively. The large variations in the values of these parameters were due to the high variability in aerosol loadings and chemical compositions of particles. Whereas the extinction coefficients were higher than observed for European and U.S. city air, they were lower than recent figures for Asian cities.[37,38,40]

For externally mixed aerosols, the single scattering albedo ω_0 varied from 0.61 to 0.87, with a mean value of 0.72 ± 0.08. Compared to most figures in the literature, for which $\omega_0 > 0.80$, magnitudes computed here are lower, due largely to high concentrations of absorbing soot particles observed by SEM. Motor vehicles, industries and domestic fuel burning are the largest contributors of particulate matter to the Cape Town atmosphere. The relatively low ω_0 values indicate also a high concentration of soot particles, demonstrating apparent differences in emission control regulations between Europe, the U.S. and South Africa. The values of σ_{ep} and ω_0 also demonstrate and explain quantitatively the reduction in visibility due to particles in the Cape Town atmosphere—the source of the city's notorious brown haze.

Environments polluted with combustion-generated aerosols, organic carbon and nitrate particles play significant roles in light scattering and absorption. Such particles could not be distinguished on the basis of morphology in the scanning electron microscope only, and hence their respective roles remain in doubt. As emission inventories of Cape Town's air listed significant emissions of organic carbon and nitrate precursors,[4] future studies need to address more closely the role of these elements in the city's brown haze, and reduce uncertainties about the nature of the particle group identified only as 'others' in this study.

P. Gwaze acknowledges the scholarship provided by the Max-Planck-Gesellschaft and a post-doctoral fellowship granted by the National Research Foundation. Additional financial support of post-doctoral studies from the University of Johannesburg is also acknowledged. Part of this work was completed by P.G. while registered for a Ph.D. in the School of Geosciences, University of the Witwatersrand, Johannesburg. Aerosol measurements in the Cape Town Brown Haze Project II were carried out together with the Climatology Research Group of the University of the Witwatersrand, using the Aerocommander 690 of the South African Weather Service. The project was funded by the South African Petroleum Industries Association and Cape Town Metro.

Received 8 September. Accepted 8 December 2006.

1. Zunckel M., John J. and Naidoo M. (2006). *The National Air Quality Management Programme (NAQMP), Output c.1., Air Quality Information Review. A Report for Directorate Environmental Information and Reporting, Environmental Quality and Protection Chief Directorate: Air Quality Management & Climate Change.* Environmentek, CSIR, Pretoria.
2. Statistics South Africa (2001). South African Census 2001. Online: http://www.statssa.gov.za/census01/html/default.asp
3. Pineda C.A. and de Villiers M.G. (1995). Air pollution study in the Cape Town area by proton-induced X-ray emission spectroscopy. *S. Afr. J. Chem.* **48**, 90–93.
4. Wicking-Baird M.C., de Villiers M.G. and Dutkiewicz R.K. (1997). *Cape Town Brown Haze Study,* Report No. Gen. 182. Energy Research Institute, University of Cape Town.
5. Jury M., Tegen A., Ngeleza E. and Dutoit M. (1990). Winter air pollution episodes over Cape Town. *Bound. Lay. Meteorol.* **53**, 1–20.
6. Piketh S.J., Otter L.B., Burger R.P., Walton N., van Nierop M.A., Bigala T., Chiloane K.E. and Gwaze P. (2004). *Cape Town Brown Haze II Report.* Climatology Research Group, University of the Witwatersrand, Johannesburg.
7. City of Cape Town (2002). *State of Environment Report Year 5, 2002,* Air Quality Monitoring Network. Online: http://www.capetown.gov.za/airqual/
8. Nel A. (2005). Air pollution-related illness: effects of particles. *Science* **308**, 804–806.
9. Eck T.F., Holben B.N., Dubovik O., Smirnov A., Goloub P., Chen H.B., Chatenet B., Gomes L., Zhang X.Y., Tsay S-C., Ji Q., Giles D. and Slutsker I. (2005). Columnar aerosol optical properties at AERONET sites in central eastern Asia and aerosol transport to the tropical mid-Pacific. *J. Geophys. Res.* **110**, D06202, doi:10.1029/2004JD005274.
10. Gwaze P. (2006). *Physical and chemical properties of aerosol particles in the troposphere: an approach from microscopy methods.* Ph.D. thesis, University of the Witwatersrand, Johannesburg.
11. Walton N.M. (2005). *Characterisation of Cape Town Brown Haze.* M.Sc. thesis, University of the Witwatersrand, Johannesburg.
12. Chiloane K.E. (2005). *Volatile organic compounds (VOCs) analysis from Cape Town Brown Haze II Study.* M.Sc. thesis, University of the Witwatersrand, Johannesburg.
13. Ebert M., Weinbruch S., Rausch A., Gorzawski G., Hoffmann P., Wex H. and Helas G. (2002). Complex refractive index of aerosols during LACE 98 as derived from the analysis of individual particles. *J. Geophys. Res.* **107**, 8121, doi:10.1029/2000JD000195.
14. Annegarn H.J., Flanz M., Kenntner T., Kneen M.A., Helas G. and Piketh S.J. (1996). Airborne streaker sampling for PIXE analysis. *Nucl. Instr. Meth. B* **109/110**, 548–550.
15. Liu Y. and Daum P.H. (2000). The effect of refractive index on size distributions and light scattering coefficients derived from optical particle counters. *J. Aerosol. Sci.* **31**, 945–957.
16. Pósfai M., Gelencsér A., Simonics R., Arató K., Li J., Hobbs P.V. and Buseck P.R. (2004). Atmospheric tar balls: particles from biomass and biofuel burning. *J. Geophys. Res.* **109**, D06213, doi:10.1029/2003JD004169.
17. Mallet M., Roger J.C., Despiau S., Putaud J.P. and Dubovik O. (2004). A study of the mixing state of black carbon in urban zone. *J. Geophys. Res.* **109**, D04202, doi:10.1029/2003JD003940.
18. Hasegawa S. and Ohta S. (2002). Some measurements of the mixing state of soot-containing particles at urban and non-urban sites. *Atmos. Environ.* **36**, 3899–3908.
19. Neusüß C., Wex H., Birmili W., Wiedensohler A., Koziar C., Busch B., Brüggemann E., Gnauk T., Ebert M. and Covert D.S. (2002). Characterization and parameterization of atmospheric particle number-, mass-, and chemical-size distributions in central Europe during LACE 98 and MINT. *J. Geophys. Res.* **107**, 8127, doi:10.1029/2001JD000514.
20. Ebert M., Weinbruch S., Hoffmann P. and Ortner H.M. (2004). The chemical composition and complex refractive index of rural and urban influenced aerosols determined by individual particle analysis. *Atmos. Environ.* **38**, 6531–6545.
21. Li J., Pósfai M., Hobbs P.V. and Buseck P.R. (2003). Individual aerosol particles from biomass burning in southern Africa: 2. Composition and aging of inorganic particles. *J. Geophys. Res.* **108**, 8484, doi:10.1029/2002JD002310.
22. Baumbach G. (1996). *Air Quality Control.* Springer-Verlag, Berlin, Heidelberg.
23. Buseck P.R. and Pósfai M. (1999). Airborne minerals and related aerosol particles: effects on climate and the environment. *Proc. Natl Acad. Sci. U.S.A.* **96**, 3372–3379.
24. Ikegami M., Okada K., Zaizen Y., Tsutsumi Y., Makino Y., Jensen J.B. and Gras J.L. (2004). The composition of aerosol particles in the middle troposphere over

the western Pacific Ocean: aircraft observations from Australia to Japan, January 1994. *Atmos. Environ.* **38**, 5945–5956.

25. Hara K., Yamagata S., Yamanouchi T., Sato K., Herber A., Iwasaka Y., Nagatani M. and Nakata H. (2003). Mixing states of individual aerosol particles in spring Arctic troposphere during ASTAR 2000 campaign. *J. Geophys. Res.* **108**, 4209, doi:10.1029/2002JD002513.
26. Seinfeld J.H. and Pandis S.N. (1998). *Atmospheric Chemistry and Physics: From Air Pollution to Climate Change.* Wiley-Interscience, New York.
27. Norman A-L., Belzer W. and Barrie L. (2004). Insights into the biogenic contribution to total sulphate in aerosol and precipitation in the Fraser Valley afforded by isotopes of sulphur and oxygen. *J. Geophys. Res.* **109**, D05311, doi:10.1029/2002JD003072.
28. South African Weather Service (2003). *Daily Weather Bulletin August 2003.*
29. Baumgardner D., Raga G.B., Kok G., Ogren J., Rosas I., Báez A. and Novakov T. (2000). On the evolution of aerosol properties at a mountain site above Mexico City. *J. Geophys. Res.* **105**, 22243–22253.
30. Horvath H. (1993). Atmospheric light absorption – a review. *Atmos. Environ. A* **27**, 293–317.
31. d'Almeida G., Koepke P. and Shettle E. (1991). *Atmospheric Aerosols. Global Climatology and Radiative Characteristics.* A. Deepak, Hampton.
32. Tegen I., Lacis A.A. and Fung I. (1996). The influence on climate forcing of mineral aerosols from disturbed soils. *Nature* **380**, 419–422.
33. Horvath H. (1998). Influence of atmospheric aerosols upon the global radiation balance. In *Atmospheric Particles,* eds R.M. Harrison and R.E. van Grieken, pp. 543–596. Wiley-Interscience, New York.
34. Formenti P., Boucher O., Reiner T., Sprung D., Andreae M.O., Wendisch M., Wex H., Kindred D., Tzortziou M., Vasaras A. and Zerefos C. (2002). STAAARTE-MED 1998 summer airborne measurements over the Aegean Sea 2. Aerosol scattering and absorption, and radiative calculations. *J. Geophys. Res.* **107**, 4451, doi:10.1029/2001JD001536.
35. Wiscombe W.J. (1980). Improved Mie scattering algorithms. *Appl. Opt.* **19**, 1505–1509.
36. Mallet M., Roger J.C., Despiau S., Dubovik O. and Putaud J.P. (2003). Microphysical and optical properties of aerosol particles in urban zone during ESCOMPTE. *Atmos. Res.* **69**, 73–97.
37. Carrico C.M., Bergin M.H., Xu J., Baumann K. and Maring H. (2003). Urban aerosol radiative properties: measurements during the 1999 Atlanta Supersite Experiment. *J. Geophys. Res.* **108**, 8422, doi:10.1029/2001JD001222.
38. Mallet M., Van Dingenen R., Roger J.C., Despiau S. and Cachier H. (2005). In situ airborne measurements of aerosol optical properties during photochemical pollution events. *J. Geophys. Res.* **110**, D03205, doi:10.1029/2004JD005139.
39. Malm W.C., Sisler J.F., Huffman D., Eldred R.A. and Cahill T.A. (1994). Spatial and seasonal trends in particle concentration and optical extinction in the United Sates. *J. Geophys. Res.* **99**, 1347–1370.
40. Bergin M.H., Cass G.R., Xu J., Fang C., Zeng L.M., Yu T., Salmon L.G., Kiang C.S., Tang X.Y., Zhang Y.H. and Chameides W.L. (2001). Aerosol radiative, physical, and chemical properties in Beijing during June 1999. *J. Geophys. Res.* **106**, 17969–17980.
41. Reid J.S., Eck T.F., Christopher S.A., Hobbs P.V. and Holben B. (1999). Use of the Ångstrom exponent to estimate variability of optical and physical properties of aging smoke particles in Brazil. *J. Geophys. Res.* **104**, 27473–27489.
42. Tang I N. (1996). Chemical and size effects of hygroscopic aerosols on light scattering coefficients. *J. Geophys. Res.* **101**, 19245–19250.
43. Weingartner E., Burtscher H. and Baltensperger U. (1997). Hygroscopic properties of carbon and diesel soot particles. *Atmos. Environ.* **31**, 2311–2327.
44. Bundke U., Hänel G., Horvath H., Kaller W., Seidl S., Wex H., Wiedensohler A., Wiegner M. and Freudenthaler V. (2002). Aerosol optical properties during the Lindenberg Aerosol Characterization Experiment (LACE 98). *J. Geophys. Res.* **107**, 8123, doi:10.1029/2000JD000188.
45. Reus de M., Formenti P., Ström J., Krejci R., Müller D., Andreae M.O. and Lelieveld J. (2002). Airborne observations of dry particle absorption and scattering properties over the northern Indian Ocean. *J. Geophys. Res.* **107**, 8002, doi:10.1029/2002JD002304.
46. Russell P.B., Redemann J., Schmid B., Bergstrom R.W., Livingston J.M., McIntosh D.M., Ramirez S.A., Hartley S., Hobbs P.V., Quinn P.K., Carrico C.M., Rood M.J., Öström E., Noone K.J., Hoyningen-Huene von W. and Remer L. (2002). Comparison of aerosol single scattering albedos derived by diverse techniques in two North Atlantic experiments. *J. Atmos. Sci.* **59**, 609–619.
47. Kittelson D.B. (1998). Engines and nanoparticles: a review. *J. Aerosol Sci.* **29**, 575–588.